



NRC Publications Archive Archives des publications du CNRC

Magnetically controlled dielectrophoresis of metallic colloids

Clime, Liviu; Veres, Teodor

This publication could be one of several versions: author's original, accepted manuscript or the publisher's version. /
La version de cette publication peut être l'une des suivantes : la version prépublication de l'auteur, la version
acceptée du manuscrit ou la version de l'éditeur.

For the publisher's version, please access the DOI link below. / Pour consulter la version de l'éditeur, utilisez le lien
DOI ci-dessous.

Publisher's version / Version de l'éditeur:

<http://dx.doi.org/10.1016/j.jcis.2008.06.032>

Journal of Colloid and Interface Science, 326, 2, pp. 511-516, 2008

NRC Publications Record / Notice d'Archives des publications de CNRC:

<http://nparc.cisti-icist.nrc-cnrc.gc.ca/npsi/ctrl?action=rtoc&an=11707535&lang=en>

<http://nparc.cisti-icist.nrc-cnrc.gc.ca/npsi/ctrl?action=rtoc&an=11707535&lang=fr>

Access and use of this website and the material on it are subject to the Terms and Conditions set forth at

http://nparc.cisti-icist.nrc-cnrc.gc.ca/npsi/jsp/nparc_cp.jsp?lang=en

READ THESE TERMS AND CONDITIONS CAREFULLY BEFORE USING THIS WEBSITE.

L'accès à ce site Web et l'utilisation de son contenu sont assujettis aux conditions présentées dans le site

http://nparc.cisti-icist.nrc-cnrc.gc.ca/npsi/jsp/nparc_cp.jsp?lang=fr

LISEZ CES CONDITIONS ATTENTIVEMENT AVANT D'UTILISER CE SITE WEB.

Contact us / Contactez nous: nparc.cisti@nrc-cnrc.gc.ca.





Magnetically controlled dielectrophoresis of metallic colloids

L. Clime*, T. Veres

NRC, Industrial Materials Institute, 75 Boulevard de Mortagne, Boucherville, Canada J4B 6Y4

ARTICLE INFO

Article history:

Received 30 April 2008

Accepted 14 June 2008

Available online 24 July 2008

Keywords:

Dielectrophoresis
Metallic colloids
Magnetic nanowires
Nanoassembly
Numerical modeling

ABSTRACT

We present a finite-element/discrete-element numerical model for calculating full trajectories of cylindrical metallic colloids in liquid flows and subjected to non-uniform electric fields. The effect of the particle orientation relative to the liquid flow is investigated by considering barcode magnetic nanowires pinned in different directions by applying uniform magnetic fields. We compare the motion of free as well as vertically and horizontally pinned nanowires and demonstrate that their nanoassembly may accurately be tuned by magnetically controlling the orientation during the dielectrophoretic capture.

© 2008 Elsevier Inc. All rights reserved.

1. Introduction

Integration of multiple nanomaterials into complex nanoscale systems is one of the key issues in recent nanotechnology. Among the most promising techniques for precise manipulation and positioning of micrometer or even submicrometer sized particles in these systems is the dielectrophoresis (DEP), i.e., the actuation of small particles (generally less than 10^{-3} m in diameter) through the action of non-uniform electric fields [1]. Most convenient approaches to the nanoassembly by using DEP consist of bridging inorganic nanowires across electrode gaps [2–5] as well as by using the electrorotation mechanism [6] and combinations of electrophoretic and dielectrophoretic forces [7]. These techniques were already proposed or even proved to be useful in nanoelectronics for providing small connecting wires [8,9], plasmon-conducting fibers [8], or integrating DEP of metallic nanowires in biomolecular recognition [10].

As recent advances in nanotechnology allow a continuously increasing control of the design of both particles and actuation devices, it is of great interest to develop theoretical models and numerical algorithms in order to describe the DEP motion of small particles of various shapes and sizes. The key issue in numerical modeling of DEP of small particles consists of accurate predictions of their trajectories when suspended in known liquid flows and subjected to non-uniform electric fields. This task usually needs to address several subsequent problems related to the liquid flow, actuation fields, and induced electric dipoles as well as drag forces and torques undergone by particles during their motion. The computation of the electric fields generated by arbitrary configurations

of metallic electrodes and the velocity fields corresponding to liquid flows in microchannels can both be reduced to simply Poisson or Laplace equations and solved by finite elements [11]. Moreover, some fundamental questions related to DEP forces and torques as well as the influence of size and slip boundary conditions on the drag forces acting on small colloids [12] must be taken into account.

Several experimental and theoretical works demonstrated that the basic theory of DEP and electrorotation [1,13,14] may successfully be applied to predict full trajectories [15] or equilibrium configurations (chaining) [16] of spherical dielectric beads. For particles of arbitrary shapes, analytical multipolar approaches [17] and numerical strategies [18] have already been proposed. However, numerical simulations related to the prediction of full trajectories in liquid flows are limited to carbon nanotubes [19,20] and do not take into account the effect of the particle orientation relative to the liquid flow. In this work, we present a 2D model for predicting full trajectories of metallic nanowires in low-conductive liquid flows and subjected to non-uniform electric fields. In order to analyze the influence of nanowires' orientation on their trappability, barcode cylindrical particles containing small magnetic inclusions are considered. Then, uniform magnetic fields are applied in order to tune the orientation of these nanowires relative to the liquid flow. The trajectories for free (no applied magnetic field), vertically pinned (vertical magnetic field), and horizontally pinned (horizontal magnetic field) nanowires are obtained from both rotational and translational equilibrium conditions and by neglecting any inertial effect. Although in this paper we consider a non-uniform electric field generated by a simple double-strip electrode system, the model may easily be generalized for more complicated geometries.

* Corresponding author.

E-mail address: Liviu.Clime@imi.cnr-c.gc.ca (L. Clime).

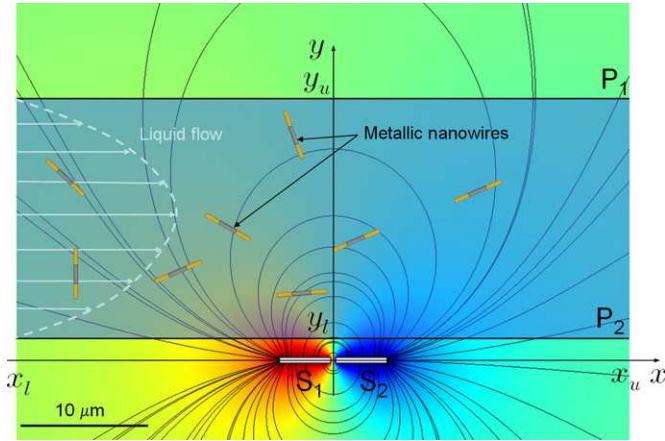


Fig. 1. Longitudinal cross section of the simulated DEP device used for electric manipulation and capture of metallic nanowires. The liquid flow is from left to right between the two plates P_1 and P_2 located at $y = y_u$ and $y = y_l$ and representing the upper and lower walls of the microfluidic channel, respectively. S_1 and S_2 represent the strip-like metallic electrodes used in order to generate the electric actuation field. Simulation domain ranges from $x = x_l$ where the nanowires are launched from up to $x = x_u$ where the untrapped particles are counted.

2. Theoretical model

We consider a laminar flow of low conductive DI water between two parallel plates P_1 and P_2 (Fig. 1) situated at $y_l = 4 \mu\text{m}$ and $y_u = 15 \mu\text{m}$ with respect to the origin of the reference frame xOy . Symmetrically with respect to the Oy axis and perpendicularly to the plane xOy there are two metallic strips S_1 and S_2 whose rectangular cross sections are $5 \mu\text{m}$ in width and $1 \mu\text{m}$ in height, with a gap between them of about $0.5 \mu\text{m}$. A non-uniform electric field is obtained by applying an electric voltage between the strips of 2 V ($+1 \text{ V}$ on S_1 and -1 V on S_2). Metallic and magnetic nanowires with different aspect ratios are launched from upstream points at $x = x_l = -15 \mu\text{m}$ and different altitudes $y_l < y < y_u$. By integrating the simultaneous translational

$$\vec{F}_{\text{el}} + \vec{F}_{\text{drag}} = 0 \quad (1)$$

and rotational

$$\vec{T}_{\text{el}} + \vec{T}_{\text{drag}} + \vec{T}_{\text{mag}} = 0 \quad (2)$$

equilibrium conditions, i.e., the conditions that the two sums of respectively all forces (electric \vec{F}_{el} and drag \vec{F}_{drag}) and all torques (electric \vec{T}_{el} , drag \vec{T}_{drag} , and magnetic \vec{T}_{mag}) be equal to zero, we determine the full trajectories and orientations of the nanowires until they either hit the bottom plate P_2 ($y < y_l$) or escape from the influence of the two strips ($x > x_u$). The integration time-dependent (unknown) variables in Eqs. (1) and (2) are the nanowire coordinates $x(t)$, $y(t)$ and nanowire orientation $\theta(t)$. Inertial effects in these equations are neglected [4] and the dependence of both force and torque terms on the integration variables is derived in the following.

The calculation of the force exerted by an electric field \vec{E} on polarizable particles is generally achieved by numerical evaluations of the Maxwell stress tensor [18]. However, when simple geometries are employed, simplified analytical expressions as

$$\vec{F}_{\text{el}} = (\vec{p} \cdot \nabla) \vec{E} \quad (3)$$

may be used in a first approximation [1,13]. Since higher order terms were omitted, the above expression is accurate only if the electric field does not significantly vary across the nanowire. Obviously, for more complicated shapes and large non-uniformities of the electric fields across the particles, multipolar representations [17] or advanced numerical methods [18] for evaluating the DEP

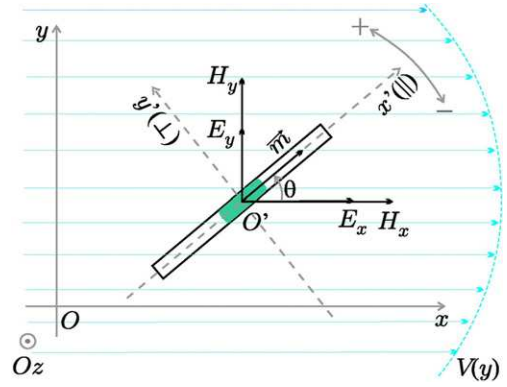


Fig. 2. Local ($x'O'y'$ -related to individual nanowires) and global (xOy -related to the microfluidic device) coordinate systems used in the equations of motion of the nanowires.

forces must be employed. The components of the dipole moment \vec{p} in Eq. (3) may be expressed as

$$\begin{cases} p_x = p_{\parallel} \cos \theta - p_{\perp} \sin \theta, \\ p_y = p_{\parallel} \sin \theta + p_{\perp} \cos \theta, \end{cases} \quad (4)$$

where p_{\parallel} and p_{\perp} are the components of the dipole moment in the local coordinate system $x'O'y'$ related to the nanowire (Fig. 2). These components depend on the nanowire polarizabilities α_{\parallel} and α_{\perp} and the local components E_{\parallel} and E_{\perp} of the applied magnetic field by

$$p_{\parallel(\perp)} = \alpha_{\parallel(\perp)} V E_{\parallel(\perp)}, \quad (5)$$

where we denoted with V the nanowire volume. In the DC (or low-frequency) limit α_{\parallel} and α_{\perp} are functions of nanowire and water conductivities only [21]

$$\alpha_{\parallel(\perp)} \cong \varepsilon_0 \varepsilon_r \frac{\sigma_p - \sigma_m}{\sigma_m + (\sigma_p - \sigma_m) L_{\parallel(\perp)}}, \quad (6)$$

where ε_0 is the vacuum absolute permittivity and ε_r the relative permittivity of the surrounding medium (water). Analytical expressions for the depolarization factors L_{\parallel} and L_{\perp} may easily be found if we consider the nanowires as prolate spheroids [22,23].

The drag force \vec{F}_{drag} acting on the nanowires will depend on their orientation relative to the liquid flow. For the sake of simplicity, we approximate again the nanowires (as we did above for the electric polarizabilities) with prolate spheroids whose semiminor and semimajor axes are equal to the radius R and half-length $L/2$ of the nanowire, respectively, and express the local components of the drag forces as

$$\vec{F}_{\text{drag},\parallel(\perp)} = 6\pi\eta R \xi_{\parallel(\perp)}(\beta) \cdot \vec{U}_{\text{rel}}, \quad (7)$$

where η is the liquid viscosity, \vec{U}_{rel} the liquid relative velocity with respect to the nanowire (that is the liquid velocity in the local coordinate system $x'O'y'$; Fig. 2), $\beta = L/2R$ the eccentricity of the nanowire, and $\xi(\beta)$ a phenomenological factor depending on its eccentricity and relative orientation to the liquid flow. Once we decide to approximate the nanowires with prolate spheroids, several analytical expressions for the functions $\xi_{\parallel(\perp)}$ are available in the literature depending on the desired accuracy or computational load [24–26]. In this paper we take

$$\xi_{\parallel(\perp)}(\beta) = \frac{4}{3} \kappa \frac{\beta^2 - 1}{A_{\parallel(\perp)} \cdot B \mp \beta}, \quad (8)$$

where

$$\begin{aligned} A_{\parallel} &= \frac{2\beta^2 - 1}{\sqrt{\beta^2 - 1}}, & A_{\perp} &= \frac{2\beta^2 - 3}{\sqrt{\beta^2 - 1}} & \text{and} \\ B &= \ln(\beta + \sqrt{\beta^2 - 1}). \end{aligned} \quad (9)$$

We introduce a phenomenological factor κ in Eq. (8) in order to account for the changes in the drag force due to the transition to the nanoscale regime [12,27]. However, we assumed here that $\kappa = 1$ as the nanowires used in our study have relatively large sizes (tens to thousands of nanometers) compared to those necessary to change the slip boundary conditions at their surface [27].

If we denote with $f_{\text{drag},\parallel(\perp)}$ the coefficient of \vec{U}_{rel} in Eq. (7) and with

$$f_{\text{drag},x} = |f_{\text{drag},\parallel} \cos \theta - f_{\text{drag},\perp} \sin \theta| \quad (10)$$

and

$$f_{\text{drag},y} = |f_{\text{drag},\parallel} \sin \theta + f_{\text{drag},\perp} \cos \theta| \quad (11)$$

the absolute values of these coefficients in the global coordinate system xOy , we may easily find from Eq. (1) that the elemental displacements of the nanowire in the directions of the global coordinate axes are

$$\Delta x = \left[V_{\text{liquid}}(y) + \frac{F_{\text{el},x}}{f_{\text{drag},x}} \right] \cdot \Delta t \quad (12)$$

and

$$\Delta y = \frac{F_{\text{el},y}}{f_{\text{drag},y}} \Delta t. \quad (13)$$

We consider a simple Poiseuille liquid flow [25] between the plates P_1 and P_2 such that the velocity $V_{\text{liquid}}(y)$ is parabolic (Fig. 1) and parallel to Ox axis. Moreover, the time interval Δt is considered small enough so that the changes in orientation relative to the liquid flow during the translation motion described by Eqs. (12) and (13) are not very important.

As the equations describing the translational motion are dependent on the orientation of the nanowires, it is very important to accurately solve Eq. (2) for the equilibrium position of the nanowire (angle θ) and the angular velocity ($\dot{\theta}$), the last parameter being responsible for the appropriate choice of the time interval Δt . It is elementary to find that Eq. (2) may be written in the form

$$\dot{\theta} = a \sin \theta + b \cos \theta + c \sin^2 \theta + d \cos^2 \theta + e \sin \theta \cos \theta, \quad (14)$$

where

$$a = -\frac{\mu_0 m H_x}{t_{\text{drag}}}, \quad b = \frac{\mu_0 m H_y}{t_{\text{drag}}}, \quad c = -\frac{(\alpha_{\parallel} - \alpha_{\perp}) V E_x E_y}{t_{\text{drag}}}, \quad (15)$$

$$d = -c \quad \text{and} \quad e = \frac{(\alpha_{\parallel} - \alpha_{\perp}) V (E_y^2 - E_x^2)}{t_{\text{drag}}}.$$

A complete derivation of Eq. (14) from Eq. (2) is presented in Appendix A. In the expression above μ_0 is the absolute vacuum magnetic permeability, m the magnetic moment of the nanowire, H_x, H_y and E_x, E_y the Cartesian components of respectively the magnetic and electric field. The quantity t_{drag} stands for the drag torque per unit angular velocity,

$$t_{\text{drag}} = \pi L^3 \eta C_r \quad (16)$$

with

$$C_r = \frac{2}{3} \frac{2 - e^2}{\frac{1+e^2}{2e^3} \ln \frac{1+e}{1-e} - \frac{1}{e^2}} \quad (17)$$

and $e = \sqrt{1 - \beta^{-2}}$ [21].

In the absence of any applied magnetic field $H_x = H_y = 0$ so that $a = b = 0$ and Eq. (14) reduces to an electrorotation problem. The absence of any applied electric field will give $c = d = e = 0$ and we have a pure magnetorotation of the nanowires. A visual comparison of these two particular processes is shown in Fig. 3 for such numerical values of the applied magnetic and electric fields

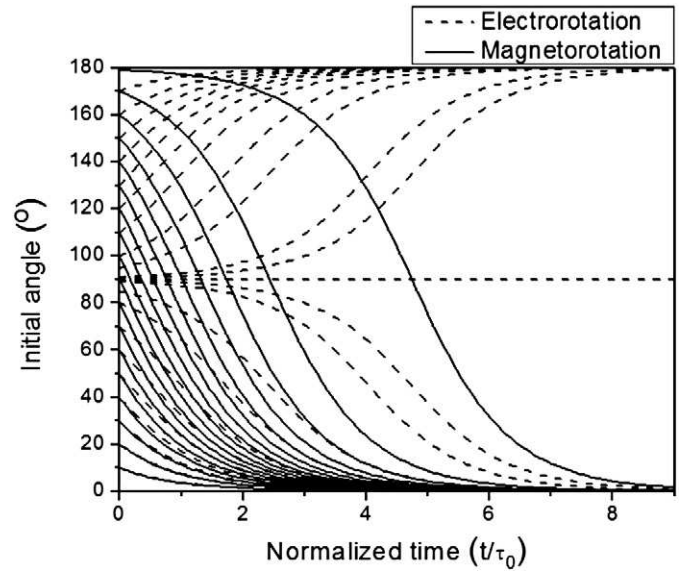


Fig. 3. Electrorotation vs magnetorotation for various initial orientations of the nanowire symmetry axis with respect to the direction of the applied field.

Table 1

Geometrical parameters (radius R and length L) of the nanowires considered in the numerical simulations

Name	R (nm)	L (nm)
NW1	40	500
NW2	80	1000
NW3	40	1000

so that $V(\alpha_x - \alpha_y)(E_x^2 + E_y^2) = \mu_0 m H$ and where Eq. (14) is numerically solved for different values of the initial angle between the magnetic moment and the field direction. The parameter τ_0 in this figure stands for the $t_{\text{drag}} / \mu_0 m H$ ratio. For analytical solutions to the electrorotation equation of nanowires (that may easily be adjusted for magnetorotation) the reader may consult Ref. [21]. However, as in the presence of both electric and magnetic fields all the coefficients in Eq. (15) are nonzero, numerical algorithms for solving ordinary differential equations (as the forth-order Runge–Kutta [28]) may become more practical.

3. Numerical simulations

The theoretical model described in the previous section was numerically implemented in order to obtain the trajectories of three types of barcode nanowires, as shown in Table 1.

All the nanowires have different aspect ratios and a magnetic moment \vec{m} which is considered parallel to their symmetry axis (Fig. 2). Both magnitudes of nanowire magnetic moments and magnetic fields are chosen so that the maximum magnetic torque (when the nanowire is perpendicular to the field) have the order of magnitude of 10^{-18} Nm. For the particular geometry of our two-strip electrode system this value is appropriate in order to align the nanowires in the direction of the magnetic field. These torques may be achieved by magnetic inclusions of several hundreds of nanometers of Ni subjected to magnetic fields of thousands of A/m.

Since the magnetic field is considered uniform, the magnetic torque acting on the magnetic nanowires depends on orientation only, being totally independent of their spatial location. This is not the case with the electric torque, as the electric field around the two strips S_1 and S_2 (Fig. 1) is non-uniform and accurate knowledge about the electric field components E_x, E_y at all the points in the liquid flow is necessary. Moreover, the computation of the

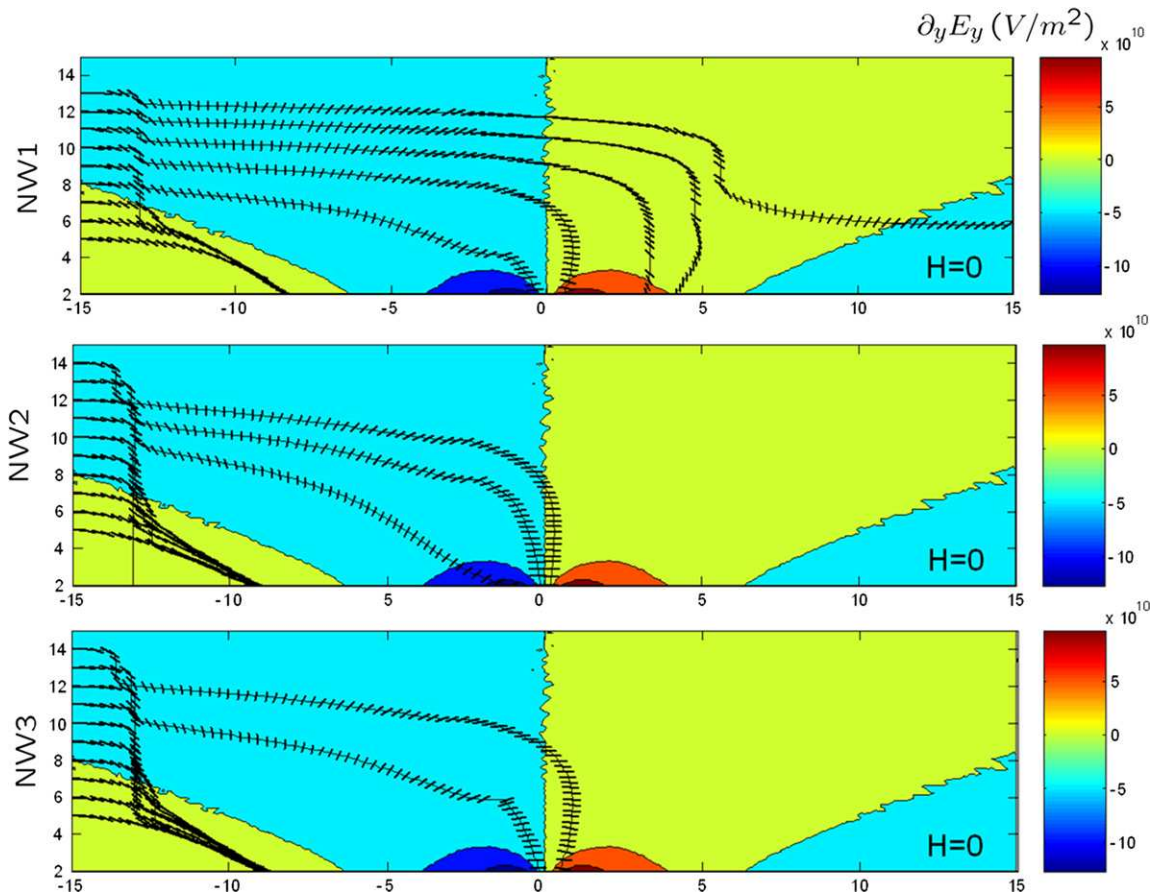


Fig. 4. Trajectories of free ($H = 0$) nanowires of different aspect ratios in a DI water flow of average velocity of $3.33 \mu\text{m/s}$. The units on axes are in micrometers.

electric force \vec{F}_{el} in Eq. (3) requires accurate values for the gradient components $\partial_x E_x$, $\partial_y E_x$, $\partial_x E_y$, and $\partial_y E_y$ of the electric field. These requirements are easily achieved when analytical functions for the electric field are available (see Ref. [19], for example) but it is more difficult when numerical algorithms are employed, due to the high order derivatives of primary variables (here the electric potential). In this paper we solve the Laplace equation ($\nabla^2 \varphi = 0$, where φ is the electric potential) corresponding to our electrode system by a finite element 2D algorithm using linear triangular mesh [11]. The corresponding solution (φ) is represented in a contour fill plot and used as background in Fig. 1. The electric field components are computed by first-order derivatives of φ on the triangular mesh whereas the components of the electric field gradient are evaluated by using an auxiliary rectangular mesh and interpolations of E_x and E_y in four neighbor nodes with polynomials of the form $c_0 + c_1x + c_2y + c_3xy$ in the least square sense [29]. The electric field gradient component $\partial_y E_y$ as well as the components E_y and E_x for the electric field are shown as contour fill plot backgrounds in Figs. 4, 5, and 6, respectively.

The nanowires are launched from upstream points in the flow at $x = x_l = -15 \mu\text{m}$ and different altitudes (y), uniformly distributed between the two plates P_1 and P_2 . As Eq. (3) is a good approximation of the dielectrophoretic force acting on particles relatively small with respect to the spatial variations of the electric field, we considered a $2\text{-}\mu\text{m}$ spacing between the electrodes and the microfluidic channel. This gap will diminish the errors due to the fact that the dimensions of the considered nanowires (Table 1) are comparable with those of the two-strip electrode system used to generate the electric field. The initial angle at the launch points is considered 0; that is, the nanowires are initially parallel to the Ox axis. Equations (1) and (2) are simultaneously solved

and both position and orientation of the nanowire updated according to Eqs. (12), (13), and (14). This strategy is applied for each type of nanowire in Table 1 and different degrees of freedom. In a first simulation we considered completely free nanowires; that is, they are moving in the absence of any applied magnetic field. As we see in Fig. 4, the orientation of these nanowires roughly follows the direction of the electric field and are attracted toward regions of high electric field gradient. However, the destination points are relatively scattered on the surface of the two electrodes. This is mainly due to the fact that the dielectrophoretic force depends not only on the gradient of the electric field but on the intensity of this field too (by increasing the induced electric dipole moment). For average liquid velocities of $3.33 \mu\text{m/s}$ all the nanowires NW1 launched at altitudes $y \leq 12 \mu\text{m}$ are trapped, the rest ($y > 12 \mu\text{m}$) being escaped. Under the same flow conditions, longer nanowires (NW2 and NW3) are totally trapped. This demonstrates that in this configuration, the increase of the drag force due to the increase of the nanowire dimensions is overwhelmed by the increase of their polarizabilities and consequently their electric moments.

Vertically pinned nanowires (Fig. 5) are expelled from the gap between the two strips but trapped onto the surface of the electrodes, where the electric field is almost vertical. On the contrary, horizontally pinned nanowires (Fig. 6) are bridging across the gap between the electrodes, where the electric field is almost horizontal. Compared to free nanowires (NW1), the trappability is decreased as only nanowires launched at altitudes lower than $9 \mu\text{m}$ are trapped. Again, as observed for free nanowires, longer and larger nanowires (NW2 and NW3) present improved trappabilities, the bigger ones (NW2) being trapped in proportion of 100% (Fig. 5).

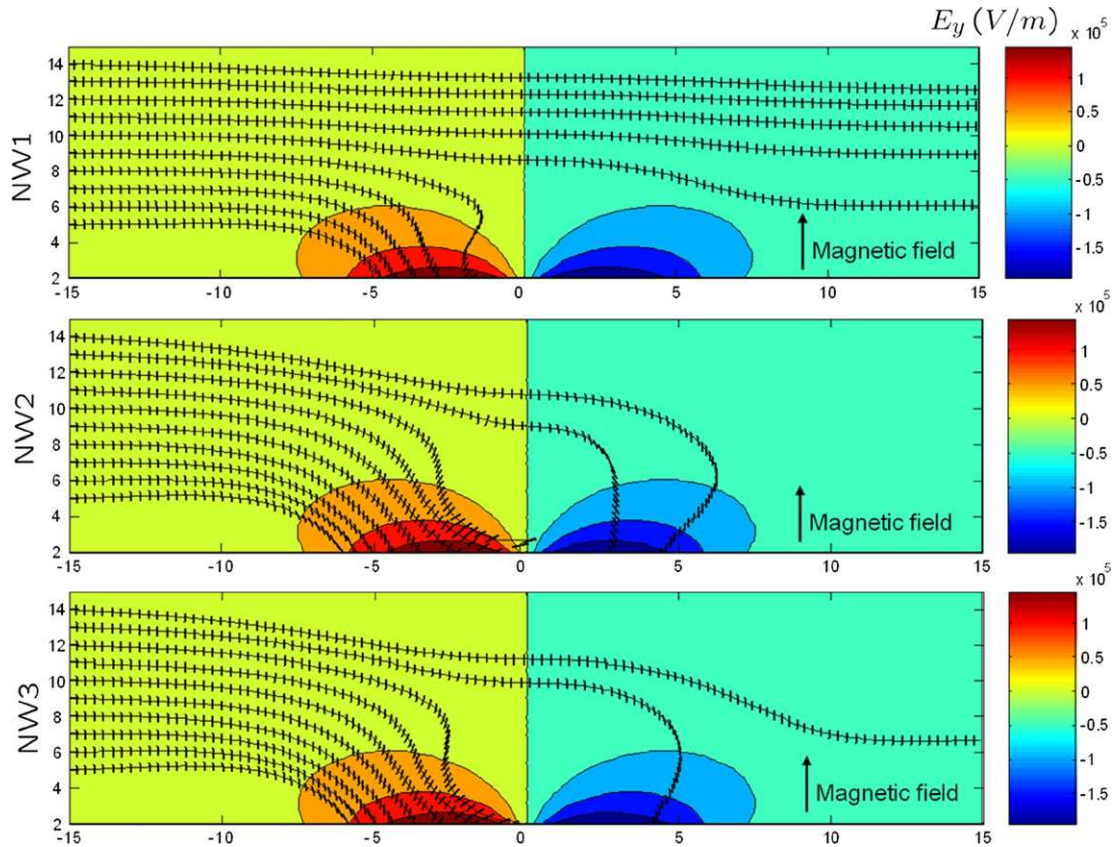


Fig. 5. Trajectories of vertically pinned ($H_x = 0$, $H_y = 100$ A/m) nanowires of different aspect ratios in a DI water flow of average velocity of $3.33 \mu\text{m/s}$. The units on axes are in micrometers.

4. Concluding remarks

Although far from being exhaustive, the present model gives an insight into the influence of the orientation of cylindrical metallic nanoparticles on their DEP manipulation and capture. Each step of these simulations may be improved in future works by more accurate evaluations of the DEP forces as well as improved phenomenological expressions for drag forces. The main advantage of the present approach is that, with some phenomenological correction factors, we can use it as a predictive tool in the design of DEP-based microfluidic devices with a minimum computational load, especially when the problem is extended into 3D.

A network of polarized micrometer-sized electrodes generates non-uniform electric fields consisting of alternating regions of horizontal and vertical field lines near the electrode gaps or their middle regions, respectively. The present simulations show that with an appropriate design of the electrode system and by controlling the orientation of the metallic colloids, improved precisions in their DEP capture may be achieved. In this work we considered noninteracting magnetic nanowires, so the magnetic interactions between both suspended and captured nanowires are completely neglected. Moreover, the electric interactions between particles are also neglected so that the presented results do not account for the mutual interactions between particles. Extension of the model in 3D for interacting barcode nanowires and a thorough experimental investigation of our theoretical predictions are planned in the near future.

Acknowledgments

The authors acknowledge Réseau Québécois de Calcul Haute Performance (RQCHP) for providing access to their computational facilities.

Appendix A. Derivation of Eq. (14)

The rotational equilibrium condition for a nanowire suspended in a liquid and subjected to electric and magnetic fields is represented by Eq. (2). If we restrict the motion of the nanowires to the plane xOy (Fig. 2) and we consider the nanowires' symmetry axis always parallel to this plane then the three vectors in Eq. (2) are perpendicular to this plane (along Oz direction) and the equilibrium reached when

$$T_{\text{drag}} = T_{\text{el}} + T_{\text{mag}}, \quad (\text{A.1})$$

that is, when the sum of clockwise and counterclockwise torques cancel each other. The above equation is in fact the scalar projection of the vectorial equilibrium condition (2) on Oz . Due to this particular restriction to the orientation of the nanowires relative to the global coordinate system, the modulus T_{el} of the electric torque $T_{\text{el}} = \vec{p} \times \vec{E}$ acting on polarizable nanowires can be simply expressed as

$$T_{\text{el}} = (p_{\parallel} E_{\perp} - p_{\perp} E_{\parallel}) \hat{z}, \quad (\text{A.2})$$

where \hat{z} is the unit vector in the direction Oz , and p_{\parallel} and p_{\perp} are the projections of the nanowire electric moment \vec{p} respectively along the nanowire symmetry axis and perpendicular on it. Similarly E_{\parallel} and E_{\perp} are the components of the electric field in the local coordinate system related to the nanowire ($x'O'y'$). These components depend on the orientation of the nanowires relative to the electrodes and consequently are unknown. A more convenient form of Eq. (A.2) can be derived if we relate these two components to E_x and E_y , corresponding to the global coordinate system xOy and directly obtained from the finite element solution of the electric field. Namely, by using

$$\begin{cases} E_{\parallel} = E_x \cos \theta + E_y \sin \theta, \\ E_{\perp} = -E_x \sin \theta + E_y \cos \theta \end{cases} \quad (\text{A.3})$$

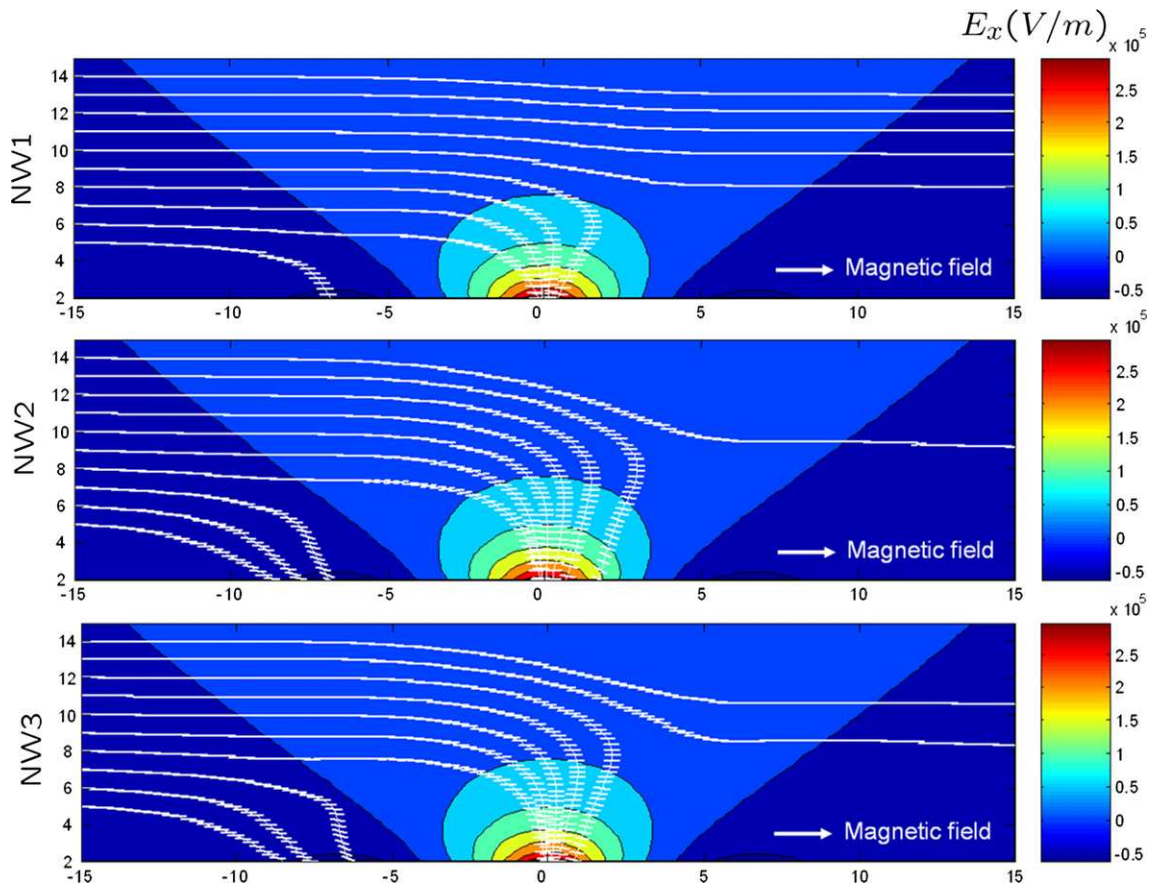


Fig. 6. Trajectories of horizontally pinned ($H_x = 100$ A/m, $H_y = 0$) nanowires of different aspect ratios in a DI water flow of average velocity of $3.33 \mu\text{m/s}$. The units on axes are in micrometers.

in (A.2) we obtain

$$T_{el} = (\alpha_{\parallel} - \alpha_{\perp})V[(E_x^2 - E_y^2) \sin \theta \cos \theta + E_x E_y (\cos^2 \theta - \sin^2 \theta)]. \quad (\text{A.4})$$

The magnetic torque $\vec{T}_{mag} = \mu_0 \vec{m} \times \vec{H}$ is also perpendicular to the plane xOy and its modulus is given by

$$T_{mag} = \mu_0 (m_x H_y \cos \theta - m_y H_x \sin \theta). \quad (\text{A.5})$$

Finally,

$$T_{drag} = t_{drag} \dot{\theta}, \quad (\text{A.6})$$

where t_{drag} is defined in Eq. (16). Using Eqs. (A.4)–(A.6) in Eq. (A.1), we obtain Eq. (14),

$$\begin{aligned} \dot{\theta} = & -\frac{\mu_0 m_y H_x}{t_{drag}} \sin \theta + \frac{\mu_0 m_x H_y}{t_{drag}} \cos \theta \\ & - \frac{V(\alpha_{\parallel} - \alpha_{\perp}) E_x E_y}{t_{drag}} \sin^2 \theta + \frac{V(\alpha_{\parallel} - \alpha_{\perp}) E_x E_y}{t_{drag}} \cos^2 \theta \\ & + \frac{V(\alpha_{\parallel} - \alpha_{\perp})(E_y^2 - E_x^2)}{t_{drag}} \sin \theta \cos \theta, \end{aligned} \quad (\text{A.7})$$

that is, a first-order ordinary differential equation (ODE) in θ .

References

- [1] T.B. Jones, *Electromechanics of Particles*, Cambridge Univ. Press, Cambridge, 1995.
- [2] J.J. Boote, S.D. Evans, *Nanotechnology* 16 (2005) 1500.
- [3] P.A. Smith, C.D. Nordquist, T.N. Jackson, T.S. Mayer, B.R. Martin, J. Mbindyo, E. Mallouk, *Appl. Phys. Lett.* 77 (2000) 1399.
- [4] D.L. Fan, F.Q. Zhu, R.C. Cammarata, C.L. Chien, *Appl. Phys. Lett.* 85 (2004) 4175.
- [5] N.I. Kovtyukhova, T.E. Mallouk, *Chem. Eur. J.* 8 (2002) 4354.
- [6] B. Edwards, T.S. Mayer, R.B. Bhiladvala, *Nano Lett.* 6 (2006) 626.
- [7] D.L. Fan, R.C. Cammarata, C.L. Chien, *Appl. Phys. Lett.* 92 (2008) 093115.
- [8] A. Graff, D. Wagner, H. Ditlbacher, U. Kreibitz, *Eur. Phys. J. D* 34 (2005) 263.
- [9] R. Beckman, E. Johnston-Halperin, Y. Luo, J.E. Green, J.R. Heath, *Science* 310 (2005) 465.
- [10] L. Shang, T.L. Clare, M.A. Erikson, M.S. Marcus, K.M. Metz, R.J. Hamers, *Nanotechnology* 16 (2005) 2846.
- [11] G. Meunier, *Modèles et formulations en électromagnétisme*, Hermès Science, Paris, 2002.
- [12] M.T. Mattews, J.M. Hill, Q. J. Mech. Appl. Math. 59 (2006) 191.
- [13] H.A. Pohl, *Dielectrophoresis*, Cambridge Univ. Press, Cambridge, 1978.
- [14] K. Foster, F.A. Sauer, H.P. Schwan, *Biophys. J.* 63 (1992) 180.
- [15] A. Al-Jarro, J. Paul, D.W.P. Thomas, J. Crowe, N. Sawyer, F.R.A. Rose, K.M. Shakesheff, *J. Phys. D Appl. Phys.* 40 (2007) 71.
- [16] J. Kadasham, P. Singh, N. Aubry, *J. Fluids Eng.* 126 (2004) 170.
- [17] T.B. Jones, M. Washizu, *J. Electrostat.* 37 (1996) 121.
- [18] A. Leonardi, G. Medoro, N. Manaresi, M. Tartagni, R. Guerrieri, *Nanotechnology* 2 (2002) 107.
- [19] M. Riegelman, H. Liu, H.H. Bau, *J. Fluids Eng.* 128 (2006) 6.
- [20] M. Dimaki, P. Boggild, *Nanotechnology* 15 (2004) 1095.
- [21] T. Itoh, S. Masuda, F. Gomi, *J. Electrostat.* 32 (1994) 71.
- [22] L.D. Landau, E.M. Lifshitz, *Electrodynamics of Continuous Media*, Pergamon Press, Oxford, 1984.
- [23] J. Venermo, A. Sihvola, *J. Electrostat.* 63 (2005) 101.
- [24] R. Byron Bird, R.C. Armstrong, O. Hassager, *Dynamics of Polymeric Liquids*, vol. 1, second ed., Wiley, New York, 1987.
- [25] J. Happel, *Low Reynolds Number Hydrodynamics: With Special Applications to Particulate Media*, Prentice-Hall, Englewood Cliffs, NJ, 1965.
- [26] A.M. Jones, J.G. Knudsen, *AIChE J.* 7 (1961) 20.
- [27] T. Sirk, Thesis, Virginia Polytechnic Institute and State University, 2006.
- [28] L.F. Samphine, *Numerical Solution of Ordinary Differential Equations*, Chapman & Hall, New York, 1994.
- [29] R.H. Bartels, J.J. Jezioranski, *ACM Trans. Math. Soft.* 11 (1985) 218.